Journal of Ovonic Research Vol. 17, No. 6, November - December 2021, p. 509 - 517

Hybrid surface plasmon polariton (SPPs) modes between metal and anisotropic plasma interface

M. Azam[a,*], A. Ghaffar[a], Y. Jamil[a], H. N. Bhatti[b]
[a]*Department of Physics, University of Agriculture, Faisalabad, Pakistan*
[b]*Department of Chemistry, University of Agriculture, Faisalabad, Pakistan*

This manuscript investigates the properties of surface plasmon polaritons (SPPs) at anisotropic plasma metal interface. It has been shown that magnetized plasma surface plasmon waves have unique features such as hybridization nature, the existence of cutoff frequency and the dependence of normalized prorogation constant and prorogation length on plasma parameters such as cyclotron frequencies (ω_c) and plasma frequency (ω_p). The influence of plasma features on normalized propagation constant and propagation as the function of frequency under different values of plasma frequency and cyclotron frequencies are studied. This suggest SPPs at magnetized plasma metal interface may be exploited for Plasma-on-Chip for cancer treatment.

(Received June 25, 2021; Accepted November 9, 2021)

Keywords: SPPs, Anisotropic Plasma, Metal,

1. Introduction

The surface plasmon polariton produce along a metal dielectric interface due to existence of unique surface EM wave is topic of great interest [1, 2]. In the certain frequency range ultraviolet (UV) to near infrared range (NIR) the real part of the permittivity of metal is negative due to collective movement of free charges and oscillate with the incident electromagnetic field [3-6]. The study on propagation of surface plasmon polariton mode along metal-dielectric interface, have attained great interest for optical community in the recent year and attracted optical research community due to its various potential uses, with switching and optical sensing, microscopy, biosensing, microscopy, integrated optics, optical devices and spontaneous quantum emitters, etc. [7, 8]. The magnetic field of SPP is purely transvers magnetic polarized wave or parallel to boundary plan [9]. In recent past years a lot of focus have been observed by researchers to take interest for involvement of anisotropic dielectrics [8, 10-12]. The optical anisotropy of dielectric gives always perpendicular to interface or transvers. These modes are basically highly dense charged waves coupling together with EM waves have ability to transmit optical signals beyond the diffraction limit through nanoscale devices. The refractive index change near metal surface is due to binding reaction with target is analyte by evanescent field of the SP mode. The detection of the optical activity of analyte is another method of optical sensing beside refractive index. The planar surface plasmon interfaces have advantages over curved geometry interfaces due least restriction in design and fabrication. Many plasmonic devices have been explored among of all these, the metal-insulator-metal planar is important component of complex nanostructure devices [6, 13-17]. Surface plasmon waveguides and filters are example of highly integrated circuit.

In material processing applications, quiescent plasmas are of great interest for reproducible surface wave. The interest in surface plasmon polariton plasma metal is limited because it was believed that is impossible to satisfy boundary conditions at these interfaces. However, experiments show that propagation of surface wave is possible along metal plasma interfaces due to fact that metal and plasma walls are not in direct contact but are separated by each other by a sheet in which plasma behave as dielectric layer [18-20]. The surface wave produced between plasma metal interface are characterized by terms of plasma parameters such as plasma electron density, collisional frequency for their exceptionally tuneability whether external

* Corresponding authors: aghaffar16@uaf.edu.pk.

magnetic field present or absent in plasma[21, 22]. The plasma material is highly desirable as compared to other dielectric materials which are expensive, difficult to handle, fragile to produce surface wave [23-28]. The scientists are eagerly engaged in advance research to improve the ability of biosensor for detection of cancer. The plasmonic devices constructed on gold films based on Nano arrays are extensively used to obtain the binding events on metal surface for optical measurement. The graphene is alternative to metal being a best conductor for generation of SPPs.

Many theoretical works reported in recent past years show the involvement of anisotropic dielectrics for SPPs generation [29-31]. These anisotropic dielectrics have optical anisotropy which led to new characteristics for example coexistence of transverse electric (TE) and transverse magnetic (TM) polarization known as hybridized SPPs with property of enhancement in prorogation length[32]. The terahertz (THz) of far infrared frequencies range have attracted many scientists for applications in spectroscopy, sensing and imaging[33-35]. The significant uses of surface wave in this regime attracted us to propose a structure composed of metal and anisotropic plasma in THz region. The characteristic equation of surface wave for different cyclotron frequencies, Plasma frequencies and metal permittivity are calculated numerically.

2. Analytical Formulations

The proposed structure shown in figure 1 consists of interface between an anisotropic plasma and a metal at x = 0 and on its top at x > 0 an anisotropic plasma while at x < 0 is metal shown in fig. 1. The metal and anisotropy of plasma are characterized by electric permittivity $\boldsymbol{\varepsilon_m}$ and $\bar{\bar{\boldsymbol{\varepsilon}}}$. In this situation the constitution relations in the permittivity tonsorial form are represented as below

$$\mathrm{D} = \varepsilon_0 \bar{\bar{\varepsilon}}.\mathrm{E} \tag{1}$$

$$\mathrm{H} = 1/\mu\mathrm{B} \tag{2}$$

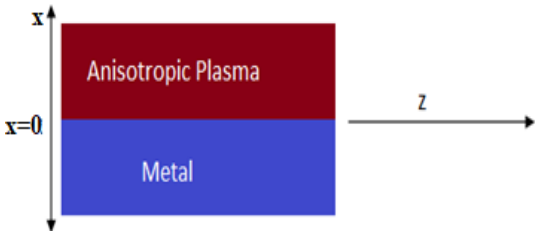

Fig. 1. Anisotropic plasma metal interface geometry.

Where H, μ and $\bar{\bar{\boldsymbol{\varepsilon}}}$ are magnetic field, free space permeability and the permittivity in tonsorial can be described as follow [36]

$$\bar{\bar{\boldsymbol{\varepsilon}}} = \begin{vmatrix} \varepsilon_1 & -\mathrm{j}\varepsilon_2 & 0 \\ j\varepsilon_2 & \varepsilon_1 & 0 \\ 0 & 0 & \varepsilon_3 \end{vmatrix} \tag{3}$$

With

$$\varepsilon_1 = \varepsilon_0 \left(1 - \frac{\omega_\mathrm{p}^2}{\omega^2 - \omega_\mathrm{p}^2}\right),$$

$$\varepsilon_2 = \varepsilon_0 \frac{\omega_\mathrm{c}\omega_\mathrm{p}^2}{\omega(\omega^2 - \omega_\mathrm{c}^2)},$$

$$\varepsilon_3 = \varepsilon_0 \left(1 - \frac{\omega_\mathrm{p}^2}{\omega^2}\right)$$

$$\omega_p = \sqrt{\frac{Ne^2}{m\varepsilon_0}},$$

and

$$\omega_c = \frac{eB_0}{m}$$

where ε_0, N, m, e and B_o are permittivity of free space, plasma density, mass of electron, electron's charge and is the external magnetic field strength. The Maxwell's equations lead to following two coupled wave equation for E_z and H_z in the anisotropic plasma [37]

$$\begin{bmatrix} \nabla_t^2 E_z \\ \nabla_t^2 H_z \end{bmatrix} + \begin{bmatrix} k_1 & jk_2 \\ jk_3 & k_4 \end{bmatrix} \begin{bmatrix} E_z \\ H_z \end{bmatrix} = 0 \tag{5}$$

where ∇_t is Laplacian in perpendicular direction,

$$k_1 = \frac{(-\beta^2 + \omega^2 \mu_0 \varepsilon_1)\varepsilon_3}{\varepsilon_1},$$
$$k_2 = \frac{\omega_p \mu \beta \varepsilon_2}{\varepsilon_1},$$
$$k_3 = -\frac{\beta \omega \varepsilon_2 \varepsilon_3}{\varepsilon_1}, \text{ and}$$
$$k_4 = \frac{\omega^2 \mu (\varepsilon_1{}^2 - \varepsilon_2{}^2)}{\varepsilon_1} - \beta^2.$$

The eigenvectors and eigen values of the 2×2 matrix in (5) gives $q_\pm^2$

$$q_\pm^2 = \frac{1}{2}\left\{k_1 + k_4 \pm \sqrt{(k_1 + k_4)^2 - 4(k_1 p_4 - k_3 k_2)}\right\} \tag{6}$$

$q_\pm$ are the wave numbers for plasma medium and β is the normalized propagation constant. The corresponding eigen-functions define the hybrid nature of the propagating modes as

$$(E_z, H_z) = (E_z, j\alpha_\pm E_z) \tag{7}$$

where $\alpha_\pm = \frac{1}{k_2}(k_1 - q_\pm^2)$ is the mode hybrid factor. In the anisotropic plasma media for the upper half space, the solutions of equation (5) are expressed

$$\left.\begin{aligned} E_z &= [U_1 e^{-q_+ x} + U_2 e^{-q_- x}] e^{-i\beta z} \\ H_z &= i\,[U_1 \alpha_+ e^{-q_+ x} + U_2 \alpha_- e^{-q_- x}] e^{-i\beta z} \end{aligned}\right\} \tag{8}$$

E_z and H_z are electric and magnetic field components for anisotropic plasma medium.

The remaining field components in the anisotropic medium can be obtained [21] as were

$$a = \frac{k_3 \omega \mu \varepsilon_2 - k_4 \beta \varepsilon_3}{\varepsilon_1 (k_1 k_4 + k_2 k_3)},$$
$$b = -\frac{\omega \mu k_3}{k_1 k_4 + k_2 k_3},$$
$$c = -\frac{k_1 \omega \mu \varepsilon_2 + k_2 \beta \varepsilon_3}{\varepsilon_1 (k_1 k_4 + k_2 k_3)},$$
$$d = -\frac{\omega \mu k_1}{k_1 k_4 + k_2 k_3},$$
$$e = -\frac{k_3 \beta}{k_1 k_4 + k_2 k_3},$$
$$f = \frac{\omega k_4 \varepsilon_3}{k_1 k_4 + k_2 k_3}$$

The lower half space ($x \lessdot 0$), i.e., metal's longitudinal field components are given as

$$\left.\begin{aligned} \mathrm{E}_z &= \mathrm{B}_1 \mathrm{e}^{\mathrm{j}\gamma \mathrm{x}} \mathrm{e}^{\mathrm{j}\beta \mathrm{z}} \\ \mathrm{H}_\mathrm{x} &= \mathrm{B}_2 \mathrm{e}^{\mathrm{j}\gamma \mathrm{x}} \mathrm{e}^{\mathrm{j}\beta \mathrm{z}} \end{aligned}\right\} \tag{9}$$

while the transverse electric (TE) field components are

$$\left.\begin{aligned} \mathrm{E}_x &= \frac{\beta}{\gamma} \mathrm{E}_\mathrm{z} \\ \mathrm{H}_\mathrm{x} &= \frac{\beta}{\gamma} \mathrm{H}_\mathrm{z} \end{aligned}\right\} \tag{10}$$

$$\left.\begin{aligned} \mathrm{E}_y &= -\frac{\omega \varepsilon_0}{\gamma} \mathrm{H}_\mathrm{z} \\ \mathrm{H}_\mathrm{y} &= -\frac{\omega \varepsilon_0}{\gamma} \mathrm{E}_\mathrm{z} \end{aligned}\right\} \tag{11}$$

where $\mathrm{A}_1, \mathrm{B}_1$, $\mathrm{A}_2$and B_2 are amplitude constants, ω is the angular frequency, ε_0 and μ_0 are the free space permittivity and permeability, $\gamma = \sqrt{\mathrm{k}_0^2 - \beta^2}$ is the decaying constant and $k_0 = \omega\sqrt{\mu_0 \varepsilon_0}$. Using the impedance boundary conditions at $x = 0$ the following characteristic relation for the anisotropic plasma–metal interface is yield as

$$\begin{aligned} \gamma q_-(-b\varepsilon_\mathrm{m}\omega + d\varepsilon_\mathrm{m}\omega\alpha_- - i(b^2 + df)\gamma\alpha_- q_+ - \mu_0\omega(f + b\alpha_-)\alpha_+ + i(b^2 + df)\gamma q_+\alpha_+) + \\ \omega\left(\mu_0\alpha_-\left(i\varepsilon_\mathrm{m}\omega + \gamma q_+(f + b\alpha_+)\right) + \varepsilon_\mathrm{m}\left(-i\mu_0\omega\alpha_+ + \gamma q_+(b - d\alpha_+)\right)\right)=0 \end{aligned} \tag{12}$$

3. Results

The proceeding section describes the characteristics of hybrid SPPs obtained from the dispersion equation (12). The dispersion equation gives the interaction and coupling of $q_\pm$ waves which are responsible of hybrid surface waves. The research results are examined numerically by computing the dispersion curves and propagation constant (β) to observe the physical behavior of hybrid SPPs. Characteristics curve study explore the behavior of the light–plasmon coupling, normalized propagation constant, attenuation or propagation loss, propagation length and the properties of SPPs waves on the semi-infinite anisotropic plasma and metal planar interface. The influence of plasma parameters such as plasma frequency which is the function of number density of electrons and cyclotron frequency which is the function magnetic field, as the function of operating surface wave frequency is reveled to explore the traits of hybrid surface wave for the xx metal (gold) and plasma waveguide structure.

Results of figure 2 depicts the influence on normalized propagation constant under the different values of plasma frequency i.e., $\omega_p = 1 * 10^9\ Hz$ (thick black), $\omega_p = 1.1 * 10^9\ Hz$ (thick orange), $\omega_p = 1.2 * 10^9\ Hz$ (thick blue) and $\omega_p = 1.3 * 10^9\ Hz$ (thick red) for the metal anisotropic plasma structure[36] . Frequency band extends from 8 to 10 GHz. It is obvious that as the plasma frequency starts increasing band gap starts squeezing but peaks of graph a shifted toward the high frequency region. Higher normalized propagation constant can be acquired at lower plasma frequencies. To explore the factor of confinement under different values of cyclotron frequency with respect to operating frequency for the proposed design is reveled in figure 3. Cyclotron frequency extends from $\omega_c = 2 * 10^6\ Hz$ to $\omega_c = 2.6 * 10^6\ Hz$ as indicated by thick black, thick orange, thick blue and thick red in figure 3. At higher operating frequencies propagation band gap starts decreasing for higher cyclotron frequencies which reflect higher normalized propagation constant can be achieved at lower cyclotron frequencies for proposed design.

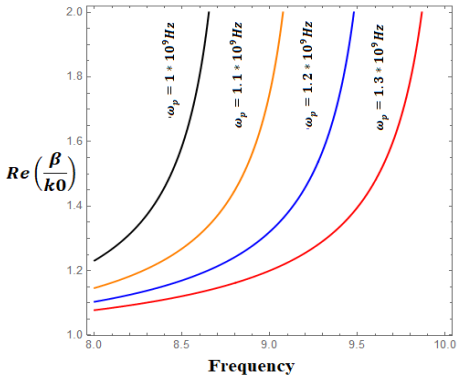

Fig. 2. Influence of plasma frequency on normalized propagation constant with respect to frequency.

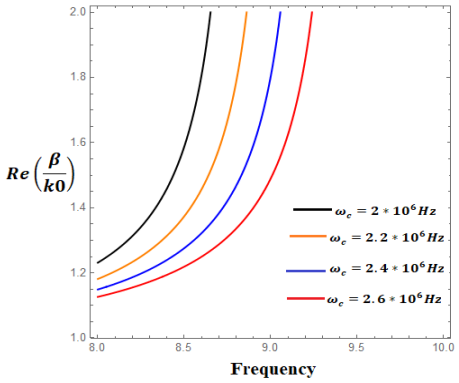

Fig. 3. Influence of cyclotron frequency on normalized propagation constant with respect to frequency.

The attenuation phase constant or propagation loss with respect to operating frequency for plasma features are revealed in figure 4 and 5. Figure 4 presents the influence on attenuation phase constant under different values of plasma frequency $\omega_p = 1 * 10^9\ Hz$ (thick black), $\omega_p = 1.1 * 10^9\ Hz$ (thick orange), $\omega_p = 1.2 * 10^9\ Hz$ (thick blue) and $\omega_p = 1.3 * 10^9\ Hz$ (thick red). it can be noted that attenuation phase constant can be tuned by tunning plasma frequency for proposed structure. Figure 5 describe the influence on attenuation phase constant under different values of cyclotron frequency i.e., $\omega_c = 2 * 10^6\ Hz$, $\omega_c = 2.2 * 10^6\ Hz$, $\omega_c = 2.4 * 10^6\ Hz$ and $\omega_c = 2 * 10^6\ Hz$ for thick black, thick orange, thick blue and thick red respectively. It can be observed that cyclotron frequency has strong impact on attenuation phase constant. The propagation length $L_p = \frac{1}{2Im\beta}$ as reported in [38] for plasma frequency and cyclotron frequency is presented 6 and 7 respectively.

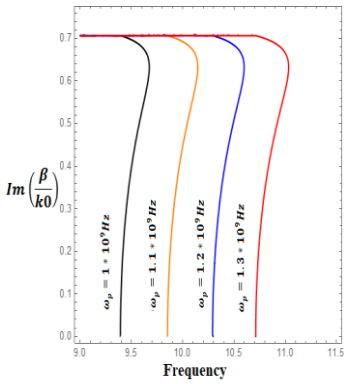

Fig. 4. Influence of plasma frequency on attenuation phase constant with respect to frequency.

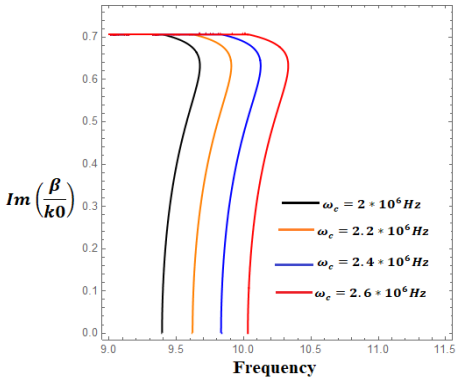

Fig. 5. Influence of cyclotron frequency on normalized attenuation phase constant with respect to frequency.

In figure 6 effect on propagation length can be seen with respect to operating frequency for different values of plasma frequency. propagation length can be increased or decreased by considerably increasing or decreasing plasma frequency for proposed design. The influence on propagation length under different cyclotron frequencies is presented in figure 7 as indicated by thick black, thick orange, thick blue and thick red. It can be seen from figure 2, 3, 4, 5, 6 and 7 that plasma features have strong effect on the propagation and modulation of hybrid surface plasmon polaritons for the proposed design which can be used for feature cutting-edge applications such as optoelectronics and nano photonic devices in the GHz frequency regime.

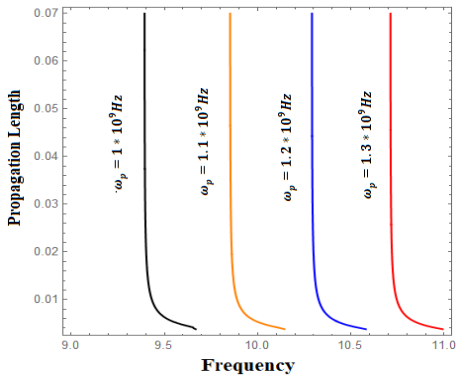

Fig. 6. Influence of plasma frequency on normalized propagation length with respect to frequency.

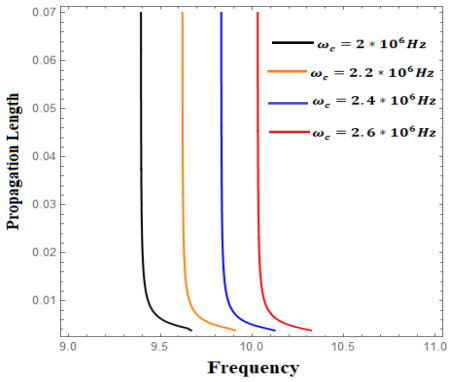

Fig. 7. Influence of cyclotron frequency on propagation length with respect to frequency.

4. Conclusion

The theoretical and numerical investigations were carried out to study the characteristics of hybrid surface waves propagating along a planar structure based on the metal–anisotropic plasma structure. The extended wave propagation theory is used to accomplish the study. The influence plasma frequency and cyclotron frequency on the normalized propagation constant, attenuation phase and propagation length are evaluated numerically.

It is concluded that plasma frequency and cyclotron frequency are very sensitive to normalized propagation constant. The plasma features (plasma frequency, cyclotron frequency) on propagation loss or attenuation phase. The propagation length an also be tuned for plasma parameters (plasma frequency, cyclotron frequency) for the proposed waveguide structure. This suggests SPPs at metal magnetized plasma interface may be exploited for Plasma-on-Chip for cancer treatment.

Acknowledgements

Authors would like to thank Higher Education Commission (HEC) under NRPU for under Project No. 8576

References

1. Krokhin, A.A., A. Neogi, and D. McNeil, *Long-range propagation of surface plasmons in a thin metallic film deposited on an anisotropic photonic crystal.* Physical Review B, 2007. **75**(23): p. 235420.
2. Berini, P., *Long-range surface plasmon polaritons.* Advances in optics and photonics, 2009. **1**(3): p. 484-588.
3. Ghaffar, A. and M.A. Alkanhal, *Electromagnetic waves in parallel plate uniaxial anisotropic chiral waveguides.* Optical Materials Express, 2014. **4**(9): p. 1756-1761.
4. Ghaffar, A., Q. Naqvi, and K. Hongo, *Study of focusing of field refracted by a cylindrical plano-convex lens into a uniaxial crystal by using Maslov's method.* Journal of Electromagnetic Waves and Applications, 2008. **22**(5-6): p. 665-679.
5. Ghaffar, A., A.A. Rizvi, and Q. Naqvi, *Fields in the focal space of symmetrical hyperboloidal focusing lens.* Progress In Electromagnetics Research, 2009. **89**: p. 255-273.
6. Yaqoob, M., et al., *Hybrid surface plasmon polariton wave generation and modulation by chiral-graphene-metal (CGM) structure.* Scientific reports, 2018. **8**(1): p. 1-9.
7. Specht, M., et al., *Scanning plasmon near-field microscope.* Physical Review Letters, 1992. **68**(4): p. 476.

8. Schultz, D.A., *Plasmon resonant particles for biological detection.* Current opinion in biotechnology, 2003. **14**(1): p. 13-22.
9. Kumara, S.A., et al., *Enhanced power conversion efficiency of the polycrystalline solar cells using spinel MnFe2O4 nanoparticles as an ARC material.* Journal of Ovonic Research Vol, 2021. **17**(5): p. 421-427.
10. Abdulhalim, I., *Surface plasmon TE and TM waves at the anisotropic film–metal interface.* Journal of Optics A: Pure and Applied Optics, 2008. **11**(1): p. 015002.
11. Gu, Y., et al., *Resonance fluorescence of single molecules assisted by a plasmonic structure.* Physical Review B, 2010. **81**(19): p. 193103.
12. Barnes, W.L., A. Dereux, and T.W. Ebbesen, *Surface plasmon subwavelength optics.* nature, 2003. **424**(6950): p. 824-830.
13. Jacob, J., et al., *Propagation of surface plasmon polaritons in anisotropic MIM and IMI structures.* Superlattices and microstructures, 2008. **44**(3): p. 282-290.
14. Apostol, M. and G. Vaman, *Plasmons and diffraction of an electromagnetic plane wave by a metallic sphere.* Progress In Electromagnetics Research, 2009. **98**: p. 97-118.
15. Manzanares-Martinez, J., *Analytic expression for the effective plasma frequency in one-dimensional metallic-dielectric photonic crystal.* Progress In Electromagnetics Research, 2010. **13**: p. 189-202.
16. Suyama, T. and Y. Okuno, *Enhancement of TM-TE mode conversion caused by excitation of surface plasmons on a metal grating and its application for refractive index measurement.* Progress In Electromagnetics Research, 2007. **72**: p. 91-103.
17. Ghaffar, A. and Q.A. Naqvi, *Focusing of electromagnetic plane wave into uniaxial crystal by a three dimensional plano convex lens.* Progress In Electromagnetics Research, 2008. **83**: p. 25-42.
18. Moisan, M. and Z. Zakrzewski, *Plasma sources based on the propagation of electromagnetic surface waves.* Journal of Physics D: Applied Physics, 1991. **24**(7): p. 1025.
19. Morita, S., et al., *Production of low-pressure planar non-magnetized plasmas sustained under a dielectric-free metal-plasma interface.* Japanese journal of applied physics, 1998. **37**(4B): p. L468.
20. Naz, M.Y., et al., *Symmetric and Asymmetric Double Langmuir Probes Characterization of Radio Frequency Inductivley Coupled Nitrogen Plasma.* Progress In Electromagnetics Research, 2011. **115**: p. 207-221.
21. Stafford, L., J. Margot, and T.W. Johnston, *Propagation of surface waves in two-plasma systems bounded by a metallic enclosure.* Journal of plasma physics, 2001. **66**(5): p. 349-362.
22. Hajijamali-Arani, Z. and B. Jazi, *Analytical formulation for the dielectric tensor and field equations of the inhomogeneous drift plasma cylinder in rotating magnetic field.* Physics of Plasmas, 2017. **24**(4): p. 042101.
23. El-Shorbagy, K.H. and H. Mahassen, *Electromagnetic wave propagation and minimizing energy losses in a rectangular waveguide filled with inhomogeneous movable plasma under the effect of a relativistic electron beam.* Indian Journal of Physics, 2019: p. 1-8.
24. Hajijamali-Arani, Z. and B. Jazi, *A description on plasma background effect in growth rate of THz waves in a metallic cylindrical waveguide, including a dielectric tube and two current sources.* Indian Journal of Physics, 2018. **92**(10): p. 1307-1318.
25. Hajijamali-Arani, Z. and B. Jazi, *An electromagnetic description for collisional drift thermal plasmas in the presence of a rotating magnetic field.* The European Physical Journal Plus, 2017. **132**(11): p. 474.
26. Arshad, K., et al., *Kinetic study of electrostatic twisted waves instability in nonthermal dusty plasmas.* Physics of Plasmas, 2017. **24**(3): p. 033701.
27. Arshad, K., M. Lazar, and S. Poedts, *Quasi-electrostatic twisted waves in Lorentzian dusty plasmas.* Planetary and Space Science, 2018. **156**: p. 139-146.
28. Arshad, K., *Application of kinetic theory to study twisted modes in non-Maxwellian plasma.* 2018.

29. Zhang, J., L. Zhang, and W. Xu, *Surface plasmon polaritons: physics and applications.* Journal of Physics D: Applied Physics, 2012. **45**(11): p. 113001.
30. Zheng, L., et al., *Experimental demonstration of surface plasmon polaritons reflection and transmission effects.* Sensors, 2019. **19**(21): p. 4633.
31. Amarie, D., et al., *Underlying Subwavelength Aperture Architecture Drives the Optical Properties of Microcavity Surface Plasmon Resonance Sensors.* Sensors, 2020. **20**(17): p. 4906.
32. Li, R., et al., *Hybridized surface plasmon polaritons at an interface between a metal and a uniaxial crystal.* Applied Physics Letters, 2008. **92**(14): p. 141115.
33. Yaqoob, M., et al., *Analysis of hybrid surface wave propagation supported by chiral metamaterial–graphene–metamaterial structures.* Results in Physics, 2019. **14**: p. 102378.
34. Yaqoob, M.Z., et al., *Characteristics of light–plasmon coupling on chiral–graphene interface.* JOSA B, 2019. **36**(1): p. 90-95.
35. Yaqoob, M., et al., *Hybrid Surface Plasmon Polariton Wave Generation and Modulation by Chiral-Graphene-Metal (CGM) Structure.* Scientific reports, 2018. **8**(1): p. 18029.
36. Gong, J., *Electromagnetic wave propagation in a chiroplasma-filled waveguide.* Journal of plasma physics, 1999. **62**(1): p. 87-94.
37. Hu, B. and C. Ruan, *Propagation properties of a plasma waveguide in an external magnetic field.* Journal of Physics D: Applied Physics, 1998. **31**(17): p. 2151.
38. Umair, M., et al., *Dispersion characteristics of hybrid surface waves at chiral-plasma interface.* Journal of Electromagnetic Waves and Applications, 2020: p. 1-13.